

Finite Element Model Updating of Buildings using Dynamic Identification Measurements



A. Scodreggio, R. Monteiro, F. Dacarro & H. Crowley

EUCENTRE, European Centre for Training and Research in Earthquake Engineering, Pavia, Italy.

R. Pinho

Department of Civil Engineering and Architecture, University of Pavia, Italy.

SUMMARY

The use of field monitoring data for seismic risk evaluation plays an important role in reducing the aleatory uncertainties, through the reconciliation between numerical and testing results or the updating of fragility functions using data available after seismic events.

Different methodologies to update FE models based on usually incomplete pre-event vibration monitoring data can be employed by minimizing a function given by the residuals between experimental and numerical quantities. The updating process should follow specific criteria, including eventual Bayesian fundamentals, so as to assure that the engineering judgment used in modeling is well kept. Furthermore, such philosophy can be extended to post-event fragility updating, based on adequate engineering demand parameters taken from nonlinear dynamic analysis of the building.

The influence of different structural parameters to be estimated on the effectiveness of the updating methodology is explored and conclusions are drawn towards the optimization of the procedure for future fragility assessment application.

Keywords: Field monitoring, FEM updating, Fragility functions, Risk assessment.

1. INTRODUCTION

In the last decade, several earthquakes produced severe damage and casualties around the world and in the European-Mediterranean region. Recent events like L'Aquila (Italy), 2009, Athens (Greece), 1999 and Izmit (Turkey), 1999, remind us that the vulnerability and exposure of our built environment are high and the seismic risk cannot be underestimated. Therefore higher protection measures should be taken to increase the resilience of our society and minimize the effects of seismic events.

One of the crucial steps for the mitigation of the seismic risk is indeed the capacity of assessing the risk and its correlated uncertainties. A unified methodology and tools for the Earthquake Engineering Community should be developed for seismic vulnerability assessment, accounting for different typologies of building and building aggregates. Within this methodology, field monitoring data will help to reduce the epistemic as well as aleatory uncertainties associated with the risk assessment procedure, allowing the creation of real time assessment tools.

The uncertainty behind any attempt to represent reality by a mathematical model is mainly caused by lack of knowledge and may exist in all aspects of the modeling procedure. Physical structural features, i.e. material, mass and geometry, are likely to be selected as updating parameters in order to improve accuracy. This process will quantify the difference between experimental and numerical results and it will subsequently modify the numerical values of the input parameters to increase the correlation between the observed dynamic response of the structure and the prediction from the numerical model.

In this paper, a methodology is presented for the numerical model updating of buildings using field monitoring data. The aim of the procedure is to find the best suitable model within a class of simulated numerical models, based on incomplete modal data, as well as the most probable value of the system natural frequencies and the full system mode shapes. A Montecarlo simulation of the structural parameters involved in the updating process is initially performed. Mean and standard deviation of the Young's Modulus, percentage of variability of the nodal masses and type of distribution of the

aforementioned sensitivity parameters among the structural members are needed in order to define the simulation of the numerical models. Changes in geometry, boundary conditions and other structural characteristics are not considered in this specific study.

The level of accuracy between measured and numerical mode shapes is estimated through the definition of a Generalized Modal Error (GME) (e.g. Alvin, 1997), which involves both frequencies and modal displacements. Finally, an elastic time-history analysis is performed so as to assure that the difference in the response between initial and updated model remained within a certain level. The proposed methodology is illustrated by updating RC frame structures with both simulated and observed modal data.

The tools that have been used for developing the aforementioned routine are Matlab, for the numerical simulations and the post-processing calculations, and OpenSees, for the structural analyses.

2. DESCRIPTION OF THE UPDATING PROCESS

The updating procedure has been schematically divided into three parts: generation of the numerical models, eigenvalue analysis and time-history analysis.

In the initial part, different simulations can be selected for the two available sensitivity parameters. Each of them considers a proper distribution of Young's Modulus and mass among the elements, according to which the Montecarlo simulation will generate the population of numerical models. Concerning the Young's Modulus simulations, four possible scenarios have been defined: the first (Figure 1) considers a single value for the overall structure; the second (Figure 2) considers one value for beams and one value for columns for the whole structure; the third (Figure 3) considers a different value for beams and columns storey-by-storey (the elastic modulus is the same for all the beams of a specific storey and it changes at each floor, same for columns) and the fourth (Figure 4) considers a different value for all the structural members, regardless of the fact that they belong to a certain level and they are beams or columns. Finally, concerning the mass simulations, the considered options were to consider a different percentage of variability for the nodal values storey-by-storey or to consider a different percentage of variability for the nodal values considering each single node. Mass can also be excluded from the simulation process, being considered in this way as a deterministic parameter.

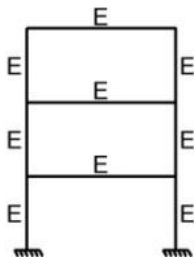


Figure 1. Young's Modulus Sim. type 1

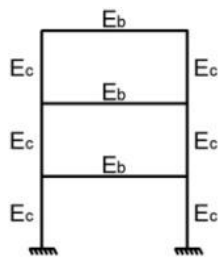


Figure 2. Young's Modulus Sim. type 2

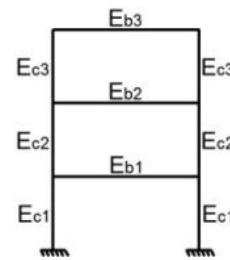


Figure 3. Young's Modulus Sim. type 3

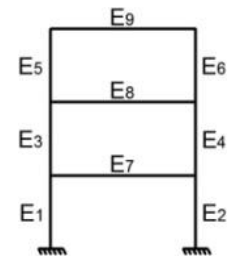


Figure 4. Young's Modulus Sim. type 4

The definition of a mean value for the characteristic compressive (cylinder) strength of concrete f_{ck} and its standard deviation is fundamental for a satisfactory matching between numerical and observed results. The aforementioned quantities are taken into account in the generation of f_{ck} values, according to a normal distribution, considering the type of Young's Modulus distribution and the number of samples which have to be generated by the algorithm.

The second part of the routine performs the modal analysis for all the numerical models which were previously simulated. Only one among them is judged as superior comparing to the initial model considered at the beginning of the updating procedure. The evaluation of a Generalized Modal Error (GME) which combines the MAC (Modal Assurance Criterion) (e.g. Alvin, 1997) index, allows the comparison between numerical responses and field monitoring data. The following formulas are used:

$$GME = \alpha_i \sum_j \frac{(\omega_j^2 - \omega_{Ei}^2)^2}{\omega_j^2} MAC_{ij} \quad (2.1)$$

$$\alpha_i = (\phi_{Ei}^T M \phi_E) \quad (2.2)$$

$$MAC_{ij} = \frac{(\phi_j^T M \phi_{Ei})^2}{(\phi_j^T M \phi_j)(\phi_{Ei}^T M \phi_{Ei})} \quad (2.3)$$

where:

- GME* Generalized Modal Error;
- ω_j eigenfrequency j from numerical model;
- ω_{Ei} eigenfrequency i from field monitoring test;
- MAC* modal assurance criterion;
- Φ_j eigenvector j from numerical model;
- Φ_{Ei} eigenvector i from field monitoring test;
- M* mass matrix;

Finally, in the third and last part of the updating routine, nonlinear dynamic analyses of initial and updated model are performed, which the purpose is to compare the elastic responses of both initial and updated model in term of displacements, to ensure that the difference of the absolute values for each of the translational DOFs doesn't exceed reasonable limits and the two responses remain comparable.

3. PRELIMINARY ANALYSES USING SIMULATED FIELD MONITORING DATA

Two preliminary tests, using structures of different degrees of geometry irregularity, were initially performed in order to calibrate the proposed methodology. The structural models, showed in Figure 5 and Figure 6, represent RC frame structures with a simple geometry and a regular distribution of stiffness and mass. Structure type 1 presents bay length of 10 m and 6 m for longitudinal and transversal direction respectively, interstorey height of 4 m and 3 m for first and second floor respectively, beam section of 0.20 m by 0.20 m and column section of 0.30 m and 0.30 m. Instead, structure type 2 presents variable bay lengths (6 m and 4 m spans) for longitudinal and transversal direction, interstorey height of 4 m for the first floor and 3 m for the upper floors and same section of 0.30 m by 0.30 m for beams and columns.

Observed field monitoring data were numerically simulated by arbitrarily changing the Young's Modulus among the structural members. No change of mass and boundary conditions are considered to simulate the field monitoring response. A notable change in the modal response was obtained, although the deformed shape for all the considered modes remained qualitatively unchanged. A comparison between the initial model (Young's Modulus equal to 30000 MPa for all the members) and the model used to obtain the observed results from field monitoring is presented in Table 1 and Table 2.

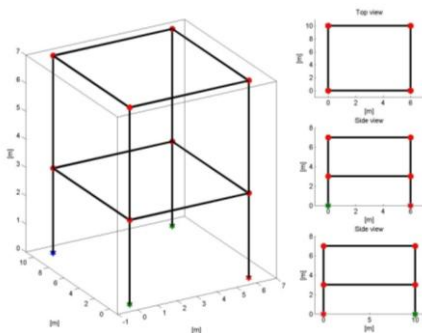


Figure 5. Test Structure 1

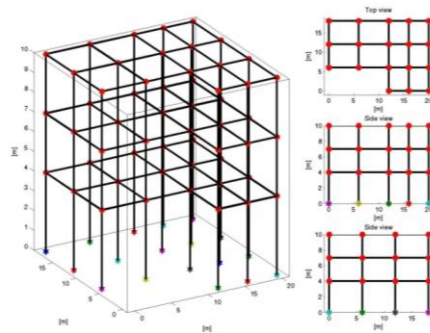


Figure 6. Test Structure 2

Table 1. Test structure 1 – Comparison between initial numerical (ω_i) and field monitoring data (ω_E)

Mode	ω_i [rad/sec]	ω_E [rad/sec]	$\Delta\omega$ [%]
1	16.95	16.64	1.82%
2	19.03	18.74	1.53%
3	20.15	19.87	1.40%
4	24.14	23.93	0.87%
5	61.54	60.87	1.08%
6	73.36	72.76	0.83%
7	79.85	78.00	2.31%
8	80.25	79.92	0.41%
9	82.50	80.83	2.02%
10	83.25	81.19	2.47%

Table 2. Test structure 2 – Comparison between initial numerical (ω_i) and field monitoring data (ω_E)

Mode	ω_i [rad/sec]	ω_E [rad/sec]	$\Delta\omega$ [%]
1	21.00	21.28	1.29%
2	21.96	22.24	1.25%
3	22.47	22.89	1.83%
4	30.89	31.18	0.93%
5	39.26	39.78	1.30%
6	45.94	46.52	1.25%
7	55.61	56.35	1.31%
8	59.96	60.58	1.03%
9	69.40	70.47	1.52%
10	71.51	72.41	1.24%

The possibility of accounting for complete measured data, i.e. considering 20 modes with 6 DOFs recorded per node, and incomplete measured data, i.e. considering 3 modes with 3 DOFs recorded per node, was investigated in these preliminary analyses. However, the type of instrumentation and the number of available instruments plays a very important role in an exhaustive and complete monitoring of the structural system. The possibility of recording only the translational DOFs, together with a limited number of instruments, not able to cover all the entire structure, leads to necessary simplifications (mode shape expansion) when analyzing the response and obtaining the modal displacements for all the structural nodes.

3.1. Calibration of the mechanical characteristic simulation

In order to obtain an adequate matching between numerical and experimental response, Montecarlo simulation has been calibrated by considering different values for mean and standard deviation of the concrete characteristic compressive strength. For the evaluation of the Young's Modulus, starting from the mean value of the concrete characteristic compressive strength f_{ck} , the formulas of the Italian Code (NTC-2008) (Decreto Ministeriale 2008) were implemented in the routine:

$$f_{cm} = f_{ck} + 8 \quad (3.1)$$

$$E_{cm} = 22000 \left(\frac{f_{cm}}{10} \right)^{0.3} \quad (3.2)$$

with:

- f_{ck} concrete characteristic compressive cylinder strength [MPa];
- f_{cm} mean value for the characteristic compressive cylinder strength [MPa];
- E_{cm} Young's Modulus [MPa];

Table 3. Type, mean and standard deviation for concrete strength

Concrete	$\mu_{f_{ck}}$ [MPa]	$\sigma_{f_{ck}}$ [MPa]
C28/35	28	8
C25/30	25	5
C20/25	22	5
C20/25	19	5
C16/20	16	5

Table 4. Upper values for the Young's Modulus simulations

$f_{ck} + \sigma_{f_{ck}}$	f_{cm} [MPa]	E_{cm} [MPa]
36	44	34313
30	38	32837
27	35	32036
24	32	31187
21	29	30279

Table 5. Lower values for the Young's Modulus simulations

$f_{ck} - \sigma_{f_{ck}}$	f_{cm} [MPa]	E_{cm} [MPa]
20	28	29962
20	28	29962
17	25	28960
14	22	27871
11	19	26672

3.2. Preliminary analysis using complete measured data

3.2.1. Test Structure 1

Several tests using complete simulated experimental data were performed for test structure 1 (Figure 5). For all those preliminary analyses, the Young's Modulus is considered as the only sensitivity parameter involved in the simulations. Distribution type 1 (Figure 1), for the aforementioned quantity, is selected. A set of six tests have been carried out by considering different mean values for the concrete compressive strength and by considering a standard deviation of 5 MPa and 8 MPa. Below, in Table 6, the list of the entire set of tests with mean and standard deviation for the sensitivity parameter, best fit model and associated Generalized Modal Error (GME) are indicated. Considering, from Table 6, the set of simulations with best performance, Figure 7 shows all the GME evaluated from the entire numerical population in which a total of 10000 models were generated.

Table 6. Set of test for Test Structure 1 with complete measured data

Test	Samples	μ_{fck} [MPa]	σ_{fck} [MPa]	Best Fit Model	GME
1.1	10000	28	8	3203	0.06065
1.3	10000	25	5	3203	0.00335
1.4	10000	22	5	5448	0.00480
1.5	10000	19	5	5081	0.00214
1.6	10000	16	5	1332	0.00172

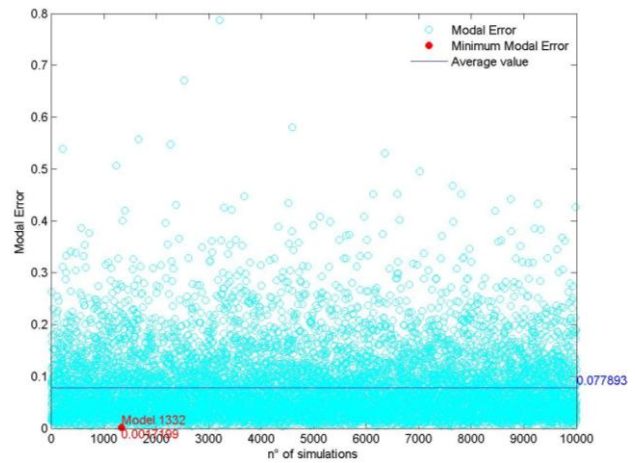


Figure 7. GME from the population of models for Test 1.6 - Test Structure 1

A first a comparison between experimental and numerical deformed shape is provided in Figure 8, Figure 9 and Figure 10. A good matching between numerical and observed response could be found.

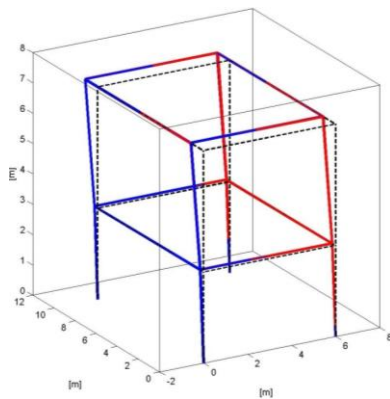


Figure 8. Exp. (red) and num. (blue) comparison - Mode 1

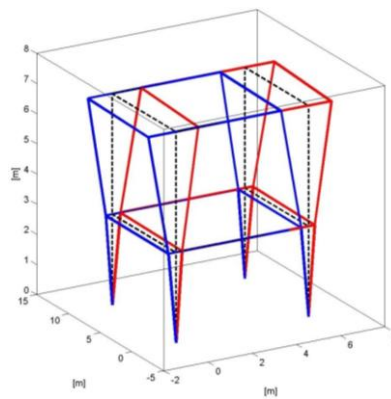


Figure 9. Exp. (red) and num. (blue) comparison - Mode 2

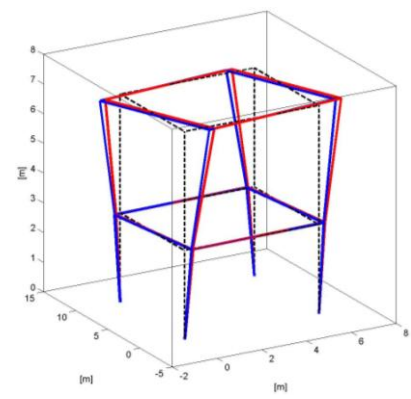


Figure 10. Exp. (red) and num. (blue) comparison - Mode 3

Regarding the comparison between experimental and numerical eigenfrequencies (Table 7), the results from the updated numerical model exhibited an improvement towards the field monitoring response with respect to the initial numerical model. In Table 8, the model from which the simulated experimental response was obtained by arbitrarily changing the Young's Modulus of the elements, is compared with initial and updated model. It can be noticed that, for several elements, updated and experimental Young's Modulus are comparable.

Table 7. Test Structure 1 - Comparison between initial (ω_i) and updated numerical (ω_U) response with complete field monitoring observations (ω_E)

Mode	ω_{Ei} [rad/s]	ω_{li} [rad/s]	ω_{Ei}/ω_{li}	ω_{Ui} [rad/s]	ω_{Ei}/ω_{Ui}
1	16.64	16.95	0.982	16.64	1.000
2	18.74	19.03	0.985	18.81	0.996
3	19.87	20.15	0.986	19.88	0.999
4	23.93	24.14	0.991	23.91	1.001
5	60.87	61.54	0.989	60.83	1.001
6	72.76	73.36	0.992	72.73	1.000
7	78.00	79.85	0.977	77.76	1.003
8	79.92	80.25	0.996	79.88	1.001
9	80.83	82.50	0.980	80.57	1.003
10	81.19	83.25	0.975	80.98	1.003

Table 8. Test Structure 1 - Comparison between initial (E_i) and updated numerical (E_U) response with complete field monitoring observations (E_E)

Elem.	E_{Ej} [kPa]	E_{ij} [kPa]	E_{Ej}/E_{ij}	E_{Uj} [kPa]	E_{Ej}/E_{ij}
1	2.8e+07	3.0e+07	0.933	27643000	1.013
2	3.1e+07	3.0e+07	1.033	27368000	1.133
3	2.7e+07	3.0e+07	0.900	28543000	0.946
4	3.2e+07	3.0e+07	1.067	26131000	1.225
5	2.7e+07	3.0e+07	0.900	28338000	0.953
6	2.7e+07	3.0e+07	0.900	29639000	0.911
7	3.0e+07	3.0e+07	1.000	29303000	1.024
8	2.6e+07	3.0e+07	0.867	29214000	0.890
9	3.0e+07	3.0e+07	1.000	31028000	0.967
10	3.0e+07	3.0e+07	1.000	30260000	0.991
11	2.9e+07	3.0e+07	0.967	30770000	0.942
12	2.9e+07	3.0e+07	0.967	29429000	0.985
13	3.0e+07	3.0e+07	1.000	30558000	0.982
14	3.0e+07	3.0e+07	1.000	30335000	0.989
15	3.1e+07	3.0e+07	1.033	29710000	1.043
16	3.0e+07	3.0e+07	1.000	29469000	1.018

3.2.1. Test Structure 2

In line with the test structure 1, distribution type 1 (Figure 1) of the Young's Modulus is selected for carrying out the updating procedure using complete simulated experimental data on test structure 2 (Figure 6). A set of six tests have been performed by considering different mean and standard deviation values for the concrete compressive strength. In Table 9, the list of the entire set of tests with mean and standard deviation values for the sensitivity parameter, best fit model and associated Generalized Modal Error (GME) are indicated. Again, considering from Table 9 the set of simulation which performed best, Table 10 shows the improvements of the updated model in matching the experimental response.

Table 9. Set of test for Test Structure 1 with complete measured data

Test	Samples	μ_{fck} [MPa]	σ_{fck} [MPa]	Best Fit Model	GME
2.1	2000	25	5	247	0.23995
2.2	2000	22	5	247	0.04642
2.3	2000	19	5	165	0.00171
2.4	2000	16	5	1332	0.02016
2.5	2000	19	8	543	0.00220
2.6	2000	19	6	1822	0.00184

Table 10. Test Structure 2 - Comparison between initial (ω_i) and updated numerical (ω_U) response with complete field monitoring observations (ω_E)

Mode	ω_{Ei} [rad/s]	ω_{li} [rad/s]	ω_{Ei}/ω_{li}	ω_{Ui} [rad/s]	ω_{Ei}/ω_{Ui}
1	21.00	21.28	0.987	20.96	1.002
2	21.96	22.24	0.987	21.93	1.001
3	22.47	22.89	0.982	22.55	0.996
4	30.89	31.18	0.991	30.73	1.005
5	39.26	39.78	0.987	39.21	1.001
6	45.94	46.52	0.987	46.07	0.997
7	55.61	56.35	0.987	55.61	1.000
8	59.96	60.58	0.990	59.91	1.001
9	69.40	70.47	0.985	69.34	1.001
10	71.51	72.41	0.988	71.66	0.998

3.3. Preliminary analysis using incomplete measured data

Taking into account the specifications and the results from the FEM updating procedures previously performed, a verification of the methodology has been done by considering incomplete simulated measured data (3 experimental mode shapes and 3 nodal DOF). The results indicate a slightly improvement in the matching between experimental and numerical modal response.

Table 11. Set of test for Test Structure 2 with incomplete measured data

Test	Samples	μ_{fck} [MPa]	σ_{fck} [MPa]	Best Fit Model	GME
1.6	10000	16	5	2133	1.40e-06

Table 13. Test Structure 1 - Comparison between initial (ω_I) and updated numerical (ω_U) response with incomplete field monitoring observations (ω_E)

Mode	ω_{Ei} [rad/s]	ω_{Ii} [rad/s]	ω_{Ei}/ω_{Ii}	ω_{Ui} [rad/s]	ω_{Ei}/ω_{Ui}
1	16.64	16.95	0.982	16.64	1.000
2	18.74	19.03	0.985	18.74	1.000
3	19.87	20.15	0.986	19.87	1.000

Table 12. Set of test for Test Structure 2 with incomplete measured data

Test	Samples	μ_{fck} [MPa]	σ_{fck} [MPa]	Best Fit Model	GME
2.3	2000	19	5	615	6.37e-06

Table 14. Test Structure 2 - Comparison between initial (ω_I) and updated numerical (ω_U) response with incomplete field monitoring observations (ω_E)

Mode	ω_{Ei} [rad/s]	ω_{Ii} [rad/s]	ω_{Ei}/ω_{Ii}	ω_{Ui} [rad/s]	ω_{Ei}/ω_{Ui}
1	21.00	21.28	0.987	20.98	1.001
2	21.96	22.24	0.987	21.96	1.000
3	22.47	22.89	0.982	22.46	1.000

4. REAL FIELD MONITORING DATA – CASE STUDY

A real building (an Elementary School building in Italy) was selected as case study for testing the methodology using real field monitoring data. In order to fulfill energy qualification of buildings, the building was monitored and a characterization of the dynamic parameters was performed.

4.1. General description of the building

The building is a 3-storey RC concrete frame structure, showed in its plan view in Figure 11. The whole building consists in three parts, divided by two seismic joints: secondary school, entrance of the building and elementary school. The dynamic identification measurements were done considering only the two edges of the building, without including the entrance. Only the part represented by the secondary school, was considered for testing the updating methodology. In the secondary school structure, all the vertical elements are continuous from the foundation to the top and the slabs are oriented along the longitudinal direction in all the entire building. The frame part is connected to the staircase (see the extreme left edge of Figure 11) which presents a wall thickness of 40 cm.

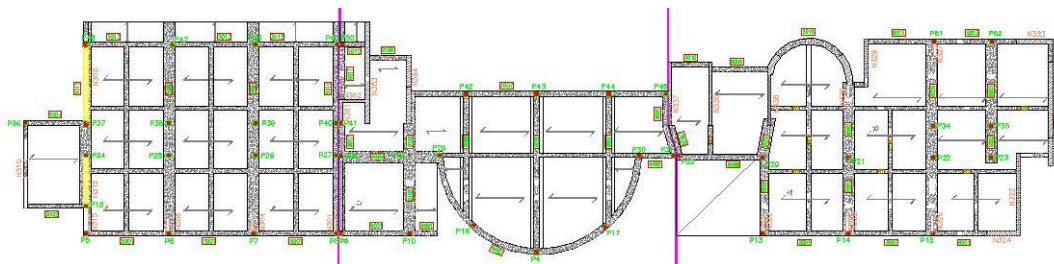


Figure 11. Plan view of the school structure (3rd level)

4.2. Dynamic identification measurements

The dynamic identification was performed considering a total of 8 tri-axial seismometers (geophones).

Table 15. Experimental modal result on the Secondary School building

Modes	T [sec]	f [Hz]	ω [rad/sec]
1 Flexural XY	0.166667	6.000	37.69911184
2 Flexural Y	0.135593	7.375	46.33849164
3 Flexural X	0.123077	8.125	51.05088062

The monitoring was done by positioning the instruments at the corners of each storey. In this way, the modal displacements of the first three eigenvectors can be reasonably assigned to the nodes at the

corners of the frame structure, for each level. Under the hypothesis of infinite stiffness in plane of the slab, only two instruments are enough to obtain the modal displacements for all the structural nodes.

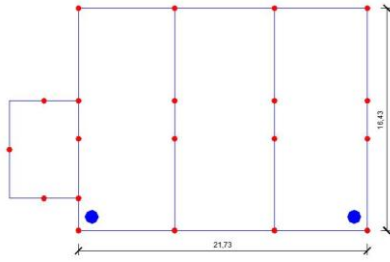


Figure 12. Geophones (blue) - Position at 1st floor

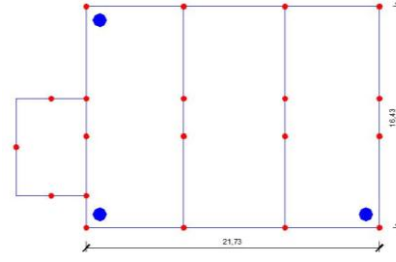


Figure 13. Geophones (blue) - Position at 2nd & 3rd floor

4.2.1 Mode shape expansion

Based on the fact that measured mode shape informations from sensor locations are fewer than the DOFs in the analytical model, mode shape expansion is employed to extrapolate the measured mode shapes such that they can be compared with the analytical numerical results. Each of the three mode shapes are obtained from the measured data by plotting the normalized measured displacements of the nodes at the corner of each storey. Consequently, the displacements of the other nodes are evaluated.

4.3 Results of the updating methodology

The analyses performed, considers three different types of parameter distribution, simulating the numerical models with one value of Young's Modulus for the entire structure, one for all the elements belonging to the same storey and a different value for each of the elements. An increasing number of generated numerical models was considered in order to understand the variability of the Generalized Modal Error (GME). No variability of the mass was taken into account for this specific case.

Table 16. Results from simulation type 1

Models	μ_{fck} [MPa]	σ_{fck} [MPa]	GME	E [kPa]
1000	18	6	1.234	3.39e+07
2000	18	6	0.261	3.49e+07
3000	18	6	0.171	3.52e+07
4000	18	6	0.137	3.53e+07
5000	18	6	0.201	3.52e+07
6000	18	6	0.167	3.53e+07
7000	18	6	0.219	3.51e+07
8000	18	6	0.171	3.52e+07

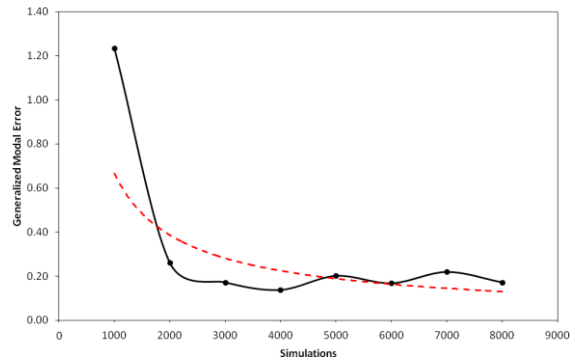


Figure 14. Variation of GME for sim. type 1

Table 17. Results from simulation type 2

Models	μ_{fck} [MPa]	σ_{fck} [MPa]	GME
1000	18	6	5.7868
2000	18	6	3.4714
3000	18	6	3.9096
4000	18	6	4.2469
5000	18	6	3.2437
6000	18	6	3.4714
7000	18	6	3.9096
8000	18	6	3.2437

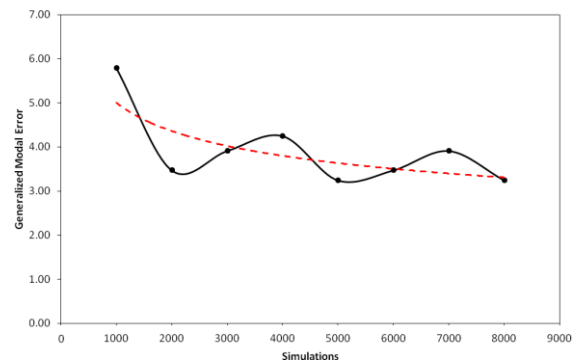
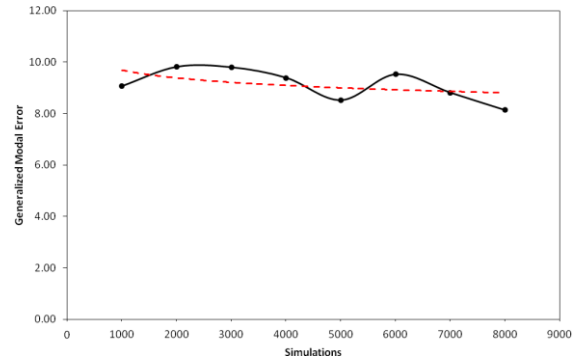


Figure 15. Variation of the GME for sim. type 2

Table 18. Results from simulation type 3

Models	μ_{fck} [MPa]	σ_{fck} [MPa]	GME
1000	18	6	9.0707
2000	18	6	9.8107
3000	18	6	9.793
4000	18	6	9.3882
5000	18	6	8.5293
6000	18	6	9.5245
7000	18	6	8.8147
8000	18	6	8.1432

**Figure 16.** Variation of the GME for sim. type 3

Simulation type 1 (Figure 14) exhibited the best results among all the analyses performed while simulation type 2 (Figure 15) and 3 (Figure 16) would probably require a higher number of simulated models for the GEM to stabilize. The curve which indicates the error index, together with the number of simulated models, rapidly decreases after a number of 2000 simulations.

One should note, though, that only the first mode was considered in the updating process, due to the fact that large discrepancies have been found between experimental and numerical deformed shapes for mode 2 and mode 3. In order to avoid this kind of uncertainty in the process, only mode 1 was taken into account for the updating of the numerical model. Considering the characteristics of the generation set yielding the best results, a calibration of the sensitivity parameter (Table 19) generation by varying mean and standard deviation of the concrete compressive strength was carried out so as to improve the matching between experimental and numerical modal response, as illustrated in Table 20 and Table 21. The updated model exhibited 0.03% of difference between numerical and experimental eigenfrequency values, while the Young's Modulus increased up to 20% respect the initial value of 30000 MPa (Table 19).

Table 19. Calibration of the sensitivity parameter (Young's Modulus) generation by varying mean and standard deviation of the concrete compressive strength

Simulation	Type	Models	μ_{fck} [MPa]	σ_{fck} [MPa]	Updated Model	GME	E [kPa]
1	1	8000	20	6	1781	0.0013138	35995000
2	1	8000	21	6	852	0.0000864	36050000
3	1	8000	22	6	759	0.0026489	35964000

Table 20. Results from calibration of the sensitivity parameter generation in term of eigenfrequencies

Simulation	Mode	ω_i [rad/s]	ω_U [rad/s]	ω_E [rad/s]	ω_i/ω_E	ω_U/ω_E
1	1	34.381	37.660	37.699	0.912	0.999
2	1	34.381	37.689	37.699	0.912	0.999
3	1	34.381	37.644	37.699	0.912	0.998

Table 21. Secondary School building - Comparison between initial (ω_i) and updated numerical (ω_U) response with incomplete field monitoring observations (ω_E)

Mode	ω_i [rad/s]	ω_U [rad/s]	ω_E [rad/s]	ω_i/ω_E	ω_U/ω_E
1	34.381	37.309	37.699	0.912	0.990

5. CONCLUDING REMARKS

The present work studied the use of dynamic identification measurements in the FE model updating of buildings. A methodology based on Montecarlo simulation scheme to update numerical models was proposed and calibrated by means of a parametric study using simulated testing structures and a real case-study.

When considering simulated field monitoring results, a good matching between experimental and numerical modal response has been encountered. Among the aforementioned analyses, the fact of considering incomplete simulated experimental data, i.e. reducing the number of modes from 20 modes up to the first three fundamental ones and considering only 3 (translational) modal DOFs per node, lead the algorithm to improve the matching with the experimental data in terms of a better comparison between experimental and numerical eigenfrequencies. Lower Generalized Modal Error values were obtained and this can be explained by the fact that a fewer number of parameters have to match the experimental quantities. However, concerning the modal deformed shape, the analysis showed poorer results comparing the same analysis using complete measured data.

In case numerical and experimental mode shapes do not correspond, such as the second and the third modes, considering the Young's Modulus as the only sensitivity parameter is not enough for matching the dynamic identification measurements. The addition of confidence parameters to the field monitoring results (e.g., through Bayesian updating), in case the detail of the information on the structure is poor, will help the algorithm to find more reliable matching of the field measurements.

Generally, the response in terms of eigenfrequencies always enabled good improvements towards the observed behaviour at the end of the updating process. However, from what it could be observed in the case-study building, the updated numerical deformed shapes didn't present a good matching with the field monitoring mode shapes. In order to overcome this problem a higher number of simulations or introducing a more efficient type of sampling at the beginning of the algorithm is needed. Latin Hypercube Sampling (LHS) might be implemented in the routine, in addition to the Montecarlo Simulation, in order to optimize the size of the samples for matching between the numerical models and experimental quantities.

The proposed updating methodology will yield more reliable models, using field monitoring data, which can be used for subsequent updating of fragility curves. This will also allow one to understand how much the changes in the properties of the numerical model will actually influence the vulnerability of the building. If a similar simulation scheme is carried out in terms of fragility analysis, a direct correlation between monitored parameters, undamaged and damaged building fragility might be sought, with the contribution of shaking table test results.

ACKNOWLEDGEMENTS

The current work was carried out under the financial auspices of the European Seventh Framework Programme (FP7) Project "NERA – Network of European Research Infrastructures for Earthquake Risk Assessment and Mitigation".

REFERENCES

- Alvin, KF. (1997). Finite element model update via bayesian estimation and minimization of dynamic residuals. *AIAA Journal* **35(5)**:, 879-886.
- Beck, JL., Vanik, MW. (1996) Structural model updating using expanded modeshapes. *Proc. 11th Engineering Mechanics Conference, ASCE, NY.* 152-155.
- Decreto Ministeriale (2008) NTC-08 Norme Tecniche per le Costruzioni (in Italian).
- Farhat, C., Hemez, PM. (1993). Updating finite element dynamics models using an element-by-element sensitivity methodology. *AIAA Journal* **31(9)**:, 1702-1711.
- Lekidis, V., Karakostas, C., Christodoulou, K., A. Karamanos, S., Papadimitriou, C., Panetsos, P. (2004). Investigation of dynamic response and model updating of instrumented R/C bridges. *13th World Conference on Earthquake Engineering, Vancouver, Canada. Paper No.* 2591.
- MathWorks, Inc (2009) MATLAB, R2009a.
- McKenna, F., Fenves, G. L., Scott, M. H., Jeremic, B. (2000). Open System for Earthquake Engineering Simulation (OpenSees). *Pacific Earthquake Engineering Research Center, University of California, Berkeley, CA.*
- Papadimitriou, C., Levine-West, M., Milman, M. (1997). Structural damage detection using modal test data. *Proc. Int. Workshop on Structural Health Monitoring, Stanford, California.*